

Evidence for a Mott-Hubbard Transition in a Two-Dimensional ^3He Fluid Monolayer

A. Casey, H. Patel, J. Nyéki, B. P. Cowan, and J. Saunders

Millikelvin Laboratory, Department of Physics, Royal Holloway University of London, Egham, Surrey, TW20 0EX, United Kingdom

(Received 15 November 2002; published 21 March 2003)

The heat capacity and magnetization of a fluid ^3He monolayer adsorbed on graphite plated with a bilayer of HD have been measured in the temperature range 1–60 mK. Approaching the density at which the monolayer solidifies into a $\sqrt{7} \times \sqrt{7}$ commensurate solid, we observe an apparent divergence of the effective mass and magnetization corresponding to a $T = 0$ Mott-Hubbard transition between a 2D Fermi liquid and a magnetically disordered solid. The observations are consistent with the Brinkman-Rice-Anderson-Vollhardt scenario for a metal-insulator transition. We observe a leading order T^2 correction to the linear term in heat capacity.

DOI: 10.1103/PhysRevLett.90.115301

PACS numbers: 67.70.+n, 67.55.-s, 71.10.Ay, 71.30.+h

The study of bulk liquid ^3He has played a central role in the development of theories of interacting Fermi systems [1]. The interatomic potential consists of a strong hard core repulsion and a weakly attractive tail. At low mK temperatures these interactions can be tuned by varying the pressure from zero to the melting pressure (34.4 bars), reducing the molar volume by approximately 30%. At sufficiently low temperatures liquid ^3He is described by Landau Fermi-liquid theory. Over this pressure range the effective mass ratio m^*/m increases from 2.80 to 5.85. The Landau parameters which are introduced phenomenologically to characterize the quasiparticle interactions have markedly different pressure dependences. F_0^s which renormalizes the compressibility increases from 9.3 to 88, but F_0^a which determines a ferromagnetic spin-spin interaction merely varies from -0.7 to -0.75 .

There is continuing interest in developing microscopic models to describe this behavior and strongly correlated Fermi systems in general. Appealing model systems are provided by two-dimensional fluid monolayers of ^3He adsorbed on atomically flat substrates. The absence of a liquid-gas transition in 2D ^3He allows the interatomic spacing in the fluid to be varied over a wide range. Thereby correlations can be tuned from weak to strong, simply by varying the surface density of ^3He atoms $n = N/A$. In this Letter we discuss a simple ^3He monolayer, subjected to a crystalline substrate potential, where it is found that the ^3He solidifies at the appropriate density into a structure commensurate with this potential. The focus here is the strong correlations in a 2D fluid which develop as its density approaches that of this commensurate solid. We argue that this provides a novel example of a metal-insulator transition in 2D, in which we can track the associated collapse of the Fermi-liquid ground state through measurements to well below the degeneracy temperature. Metal-insulator (MI) transitions continue to be the subject of widespread interest [2–4], as well as some controversy [5]. The present system seems to provide an example of a MI transition occurring via the

Brinkman-Rice-Anderson-Vollhardt scenario [6]. In the simplest model, one considers half-filling: one particle per site, and magnetic interactions are neglected. The MI transition can be regarded as a quantum phase transition arising from competition between tunneling motion, tending to reduce zero point kinetic energy, and on-site repulsion U . This model was applied by Anderson and Brinkman [7] to bulk liquid ^3He , and developed into the “almost localized fermion” model [8]. This involves introducing a fictitious lattice; the model has also been generalized away from half-filling [9]. The key results, at half-filling, are that a MI transition occurs as $U \rightarrow U_c$, while $m^*/m \rightarrow \infty$, $F_0^a \rightarrow -3/4$. The large increase in compressibility with pressure is also explained [8,10]. Recently results on the polarization dependence of the specific heat in bulk liquid ^3He have been discussed in the context of such models [11].

The advantages of our experimental system are that it is truly two dimensional, with no interlayer coupling, and it has simple short-range interactions and negligible spin-orbit coupling. A particularly interesting feature is that the solid is highly magnetically frustrated and it is believed to have a quantum spin-liquid ground state [12]. The second layer of ^3He adsorbed on bare graphite has been extensively investigated. The first layer forms a compressed 2D paramagnetic solid of density 11.2 nm^{-2} , as determined by neutron scattering [13]. The first heat capacity measurements of the second layer fluid were well described by the form $c = \beta + \gamma T$ [14], where $\gamma = \pi k_B^2 A m^*/3\hbar^2$. The β term is attributed to residual substrate heterogeneity [14,15], and A is the area of the substrate. The effective mass ratio m^*/m of the second layer fluid was found to vary from unity at the lowest densities to 4.5 at 4.4 nm^{-2} . Measurements of the magnetization found enhancements relative to that of an ideal Fermi gas up to 25 at a density of 5.4 nm^{-2} [16]. Since $M/M_0 = m^*/m(1 + F_0^a)$, these measurements together allow a determination of F_0^a . Although the effective mass increases with density, F_0^a appeared to saturate with $F_0^a \approx -3/4$, close to the value observed in bulk

liquid, consistent with the picture of liquid ^3He as an “almost localized” system.

Heat capacity measurements [14] were the first to show that the second layer solidified at a density of 6.4 nm^{-2} . It was proposed that this occurred by the formation of a triangular lattice in $\sqrt{7} \times \sqrt{7}$ commensuration with the first layer [17], and such a structure has subsequently been found in path integral Monte Carlo simulations [18]. Later measurements of the magnetization suggested that a “highly correlated regime” existed in the fluid near solidification, which began at 5.8 nm^{-2} [19,20].

In this Letter we report measurements of the heat capacity and nuclear magnetization of a fluid ^3He monolayer adsorbed on graphite plated with a bilayer of HD, in which we concentrate on the region close to solidification [21]. Since the density of each HD layer is 9.1 nm^{-2} the $\sqrt{7} \times \sqrt{7}$ solid now forms at 5.2 nm^{-2} [22]. This is a quantum solid of remarkably low density, with interparticle spacing greater than in bulk liquid ^3He at zero pressure. At fluid coverages approaching this commensurate density we observe a rapid increase in the quasiparticle effective mass that we interpret as critical behavior approaching a Mott-Hubbard transition. The magnetization diverges in a similar way indicative of F_0^a tending to a constant. The measurements were performed using an experimental cell that is described in more detail elsewhere [22]. The procedures for preplating the graphite surface with a bilayer of HD are those followed in previous work. The heat capacity data for coverages $n \leq 5.0 \text{ nm}^{-2}$ are shown in Fig. 1. At sufficiently low temperatures the data are well described by $c = \beta + \gamma T + \Gamma_{2D} T^2$. The T^2 term is the leading order correction predicted in 2D, as discussed later. At each density the effective mass ratio is inferred from fits to the data of this form, Fig. 2 [23]. It increases from close to unity at

the lowest density to around 13 at $n_3 = 5.0 \text{ nm}^{-2}$, significantly larger than the effective mass in bulk liquid at the melting pressure.

In earlier continuous wave NMR experiments performed in the same cell, we determined the magnetization enhancement relative to an ideal Fermi gas M/M_0 . Assuming the validity of the almost localized fermion model (essentially that $F_0^a \rightarrow -3/4$), we can infer values of m^*/m from the magnetization data [24]. These are also plotted in Fig. 2, and are clearly in agreement with the direct determination from the heat capacity data [25]. Within the lattice gas picture, our experimental system is actually more closely modeled by the filling controlled metal-insulator transition. Note that in the adsorbed film the ^3He is exposed to the crystalline potential of the HD substrate, but “half-filling” is never achieved because of the short-range repulsion between ^3He atoms. Rather, it is natural to take the density of the lattice as n_c , that of the commensurate solid. Then the “doping” $\delta = (1 - n/n_c)$. It is then expected that $m^*/m \sim 1/\delta$ [9]. We fit the apparent divergence of the effective mass, over the whole density range, to the empirical form $m^*/m = (1 - n/n_c)^{-\nu}$, and we find for the critical density $n_c = 5.1 \text{ nm}^{-2}$, close to the value of 5.2 nm^{-2} for the $\sqrt{7} \times \sqrt{7}$ solid. The precision does not allow a reliable determination of the critical exponent. The solid is stabilized at the commensurate density by the combined effects of the periodic potential due to the HD substrate, the short-range hard core repulsive energy between ^3He atoms, and their zero point energy. Thus correlation effects are crucial to its existence, and precursor behavior in the 2D fluid suggestive of the approach towards a critical point lead us to identify this transition as Mott-Hubbard localization. However, it appears that solidification may be

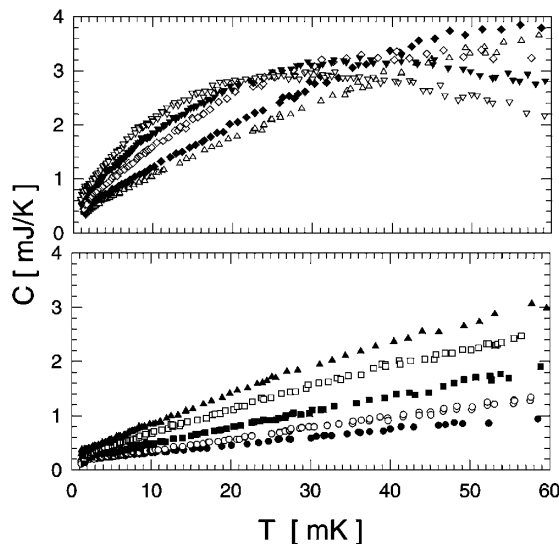


FIG. 1. Heat capacity at ^3He coverages: 1.00 (●), 2.00 (○), 3.00 (■), 4.00 (□), 4.40 (▲), 4.70 (△), 4.80 (◆), 4.90 (◇), 4.95 (▼), and 5.00 nm^{-2} (▽).

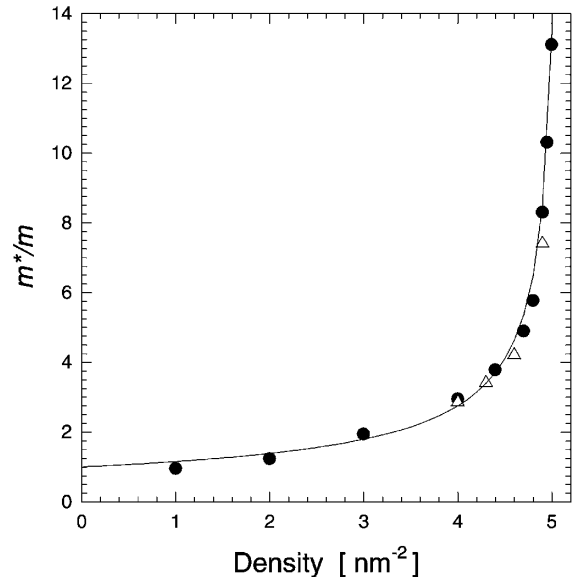


FIG. 2. Effective mass ratio as a function of ^3He fluid density inferred from heat capacity (●), magnetization (△), showing apparent divergence. Solid line is fit to data (see text).

weakly first order; heat capacity isotherms are consistent with a narrow coexistence region between 5.1 and 5.4 nm⁻². The advantage of the HD substrate is that the critical density can be approached more closely than in the second layer on bare graphite.

In passing, we note that similar behavior at a MI transition has been seen in the 3D compound Sr_{1-x}La_xTiO₃ [26] as $x \rightarrow 1$. The common feature of the insulating phase in the two cases is magnetic frustration, particularly pronounced in the case of 2D solid ³He, which is frustrated both geometrically, due to the triangular lattice, and because of competing multiple spin exchange interactions [12].

In the present case, our measurements extend into the Fermi-liquid regime even when the density is tuned close to the Mott transition. In this regime we find clear evidence that to leading order the fluid heat capacity is given by $c = \gamma T + \Gamma_{2D} T^2$, Fig. 3. The unusual T^2 term has been found theoretically by a number of authors [27–29], and this is the first clear experimental confirmation of it. It should be compared to bulk ³He, where the form $c = \gamma T + \Gamma_{3D} T^3 \ln(T/T_0)$ is found both experimentally and theoretically [30,31]. Here Γ_{3D} has been calculated within Fermi-liquid theory in terms of the Landau parameters and has a magnitude consistent with that expected for spin fluctuations. For the 2D case, both long range quasiparticle interactions and collective modes are shown to contribute to the T^2 correction [27]; elsewhere the fact that the spin fluctuation spectrum in 2D is relatively flat, with no pronounced low frequency peak, is emphasized and a T^2 correction is calculated numerically [28]. A variation of 3 orders of magnitude is observed in the measured coefficient Γ_{2D} , reflecting the wide range of effective mass ratio, which in this system varies over more than an order of magnitude. Empirically it is natural

to write the heat capacity as an expansion in T/T_F^* , where $T_F^* = T_F/(m^*/m)$; here $T_F = \pi\hbar^2 N/k_B m A$ is the Fermi temperature of an ideal Fermi gas. Then $c = \frac{1}{3} \pi^2 N k_B [\frac{T}{T_F} + \alpha \frac{T^2}{T_F^2}]$, and α is a dimensionless parameter. Figure 4 shows that $\Gamma_{2D} N$ varies as $(m^*/m)^3$; hence $\alpha \sim (m^*/m)$. Introducing a characteristic temperature $T_0 = T_F^*/\alpha$, which we can identify with the degeneracy temperature (coherence temperature) [3,4] below which the Fermi-liquid state is well defined, this result corresponds to $T_0 \sim T_F^{*2} \sim \gamma^{-2} \sim (m^*/m)^{-2}$. Thus the divergence of the effective mass implies a rapid collapse of Fermi-liquid behavior as the Mott transition is approached. To further explore the systematics of this collapse we plot in Fig. 5, for selected coverages, a reduced heat capacity coefficient versus reduced temperature T/T_F^* , where T_F^* is calculated from the known density and measured values of m^*/m . It can be seen that at 5 nm⁻², the plateau in c/T develops only below 10 mK, corresponding to $T/T_F^* \sim 0.05$. In terms of dynamical mean field theory [4], this corresponds to the disappearance of the quasiparticle peak in the density of states at the Fermi energy with increasing temperature above the degeneracy temperature. The data necessarily collapse at the lowest temperatures. However, it is clear that the reduced temperature range of the plateau shrinks as $n \rightarrow n_c$; in other words, $T_0 \rightarrow 0$ faster than $T_F^* \rightarrow 0$, consistent with the analysis from Γ_{2D} .

This behavior is found in several theoretical models. According to scaling proposed by Imada [32], $m^*/m \sim \delta^{(d-z)/d}$, while $T_0 \sim \delta^{d/z}$. Thus the experimental result for the relative scaling of T_0 and m^* is consistent with a dynamical critical exponent $z = 4$, for dimensionality $d = 2$. In this case $m^*/m \sim 1/\delta$. In contrast, dynamical mean field theory finds $T_0 \sim \delta^{3/2}$ [33]. In the coverage range from 4.8 to 5.0 nm⁻², in the regime of strongest correlations close to the Mott transition, for which the

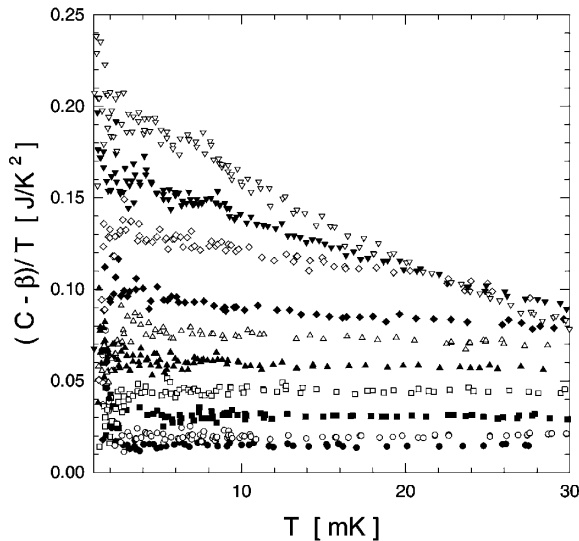


FIG. 3. Fluid heat capacity, obtained by subtracting “ β term” from total ³He heat capacity, divided by temperature, as a function of T , to illustrate T^2 correction.

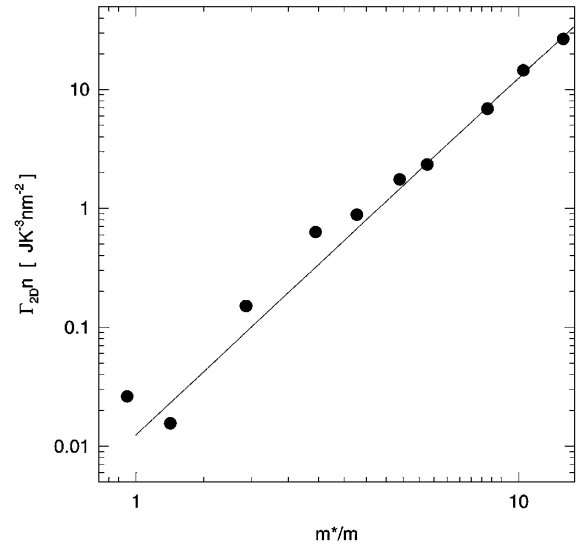


FIG. 4. $\Gamma_{2D} n$ vs m^*/m , where Γ_{2D} is a coefficient of the T^2 term and n is the number of ³He atoms per unit area.

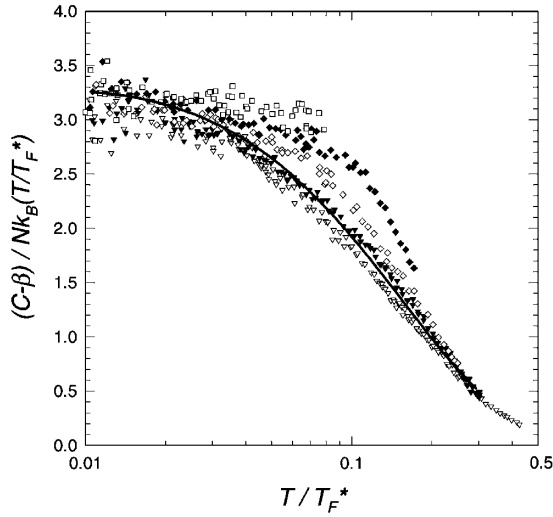


FIG. 5. Reduced fluid heat capacity as a function of reduced temperature, showing emergence of Fermi liquid at low temperatures: 3.00 (\square), 4.80 (\blacklozenge), 4.90 (\diamond), 4.95 (\blacktriangledown), and 5.00 nm⁻² (∇). Solid line, a fit to numerically calculated values of [28], with $F_0^a = -0.78$.

temperature range of measurements, shown in Fig. 1, extends well beyond the Fermi-liquid regime, we find a temperature dependence of the heat capacity consistent with the form $T \ln T$, as can be seen in Fig. 5. Such a term has been found in calculations of the spin fluctuation contribution to the heat capacity to emerge from a T^2 term above some characteristic temperature $\sim 0.1 T_F^*$ [28].

By studying a 2D ³He fluid film adsorbed on a crystalline substrate we find evidence for a Mott metal-insulator transition, between a 2D Fermi liquid and a spin disordered solid, which follows the Brinkman-Rice-Anderson-Vollhardt scenario, to be compared with the classic case of bulk ³He. It suggests that doping a magnetically frustrated Mott insulator results in a Fermi liquid. It would also be desirable to make a detailed comparison of a Fermi-liquid theory calculation of Γ_{2D} with the present data.

We particularly thank A. Millis, M. Imada, G. Kotliar, and S. Julian for valuable discussions. This work was supported by EPSRC (U.K.).

[1] D. Vollhardt and P. Wölfle, *The Superfluid Phases of Helium 3* (Taylor and Francis, London, 1990).
 [2] F. Gebhard, *The Mott Metal-Insulator Transition* (Springer, New York, 1997).
 [3] M. Imada, A. Fujimori, and Y. Tokura, Rev. Mod. Phys. **70**, 1039 (1998).
 [4] A. Georges, G. Kotliar, W. Krauth, and M. Rozenberg, Rev. Mod. Phys. **68**, 13 (1996).
 [5] R. B. Laughlin, Adv. Phys. **47**, 943 (1998), and references therein.
 [6] W. F. Brinkman and T. M. Rice, Phys. Rev. B **2**, 4302 (1970).

[7] P. W. Anderson, *Basic Notions of Condensed Matter Physics* (Benjamin, New York, 1984).
 [8] D. Vollhardt, Rev. Mod. Phys. **56**, 99 (1984).
 [9] D. Vollhardt, P. Wölfle, and P. Anderson, Phys. Rev. B **35**, 6703 (1987).
 [10] A. Georges and L. Laloux, Mod. Phys. Lett. B **11**, 913 (1997), argue that this model incorrectly includes magnetic correlations.
 [11] O. Buu, L. Puech, and P. E. Wolf, Phys. Rev. Lett. **85**, 1278 (2000).
 [12] G. Misguich, B. Bernu, C. Lhuillier, and C. Waldtmann, Phys. Rev. Lett. **81**, 1098 (1998), and references therein.
 [13] H. Godfrin and H. J. Lauter, *Progress in Low Temperature Physics* (North-Holland, Amsterdam, 1995), Vol. 14.
 [14] D. S. Greywall, Phys. Rev. B **41**, 1842 (1990).
 [15] A. Golov and F. Pobell, Phys. Rev. B **53**, 12647 (1996).
 [16] C. P. Lusher, B. P. Cowan, and J. Saunders, Phys. Rev. Lett. **67**, 2497 (1991).
 [17] V. Elser, Phys. Rev. Lett. **62**, 2405 (1989).
 [18] M. Pierce and E. Manousakis, Phys. Rev. B **59**, 3802 (1999), and references therein.
 [19] K. D. Morhard, C. Bäuerle, J. Bossey, Y. M. Bunkov, S. N. Fisher, and H. Godfrin, Phys. Rev. B **53**, 2658 (1996).
 [20] C. Bäuerle *et al.*, J. Low Temp. Phys. **110**, 333 (1998).
 [21] Preliminary reports of aspects of these results are published in A. Casey, H. Patel, J. Nyéki, B. P. Cowan, and J. Saunders, J. Low Temp. Phys. **113**, 293 (1998) and Physica (Amsterdam) **280B**, 100 (2000).
 [22] M. Siqueira, C. P. Lusher, B. P. Cowan, and J. Saunders, Phys. Rev. Lett. **71**, 1407 (1993).
 [23] We note that the value of β increases over the density range explored by a factor of ~ 3 . For $n \gtrsim 3$ nm⁻², we find $\beta \propto \ln(m^*/m)$.
 [24] Within the almost localized fermion model $1 + F_0^a = [1 + (1 - m/m^*)^{1/2}]^{-2} + \varepsilon$, where ε depends on the energy dependence of the density of states and weakly on m/m^* , here we take $\varepsilon = 0$. F_0^a is determined from the magnetization enhancement M/M_0 . Equivalently $m^*/m = (M_0/M + M/M_0 + 2)/4$. The total magnetization comprises a fluid contribution plus a contribution from localized solid that dominates at the lowest temperatures. The fluid contribution to the magnetization is fit to $M = C(T^2 + T_F^{*2})^{-1/2}$, so that $M/M_0 = T_F/T_F^{**}$, where T_F is the Fermi temperature of an ideal gas at the same density $T_F = 0.505n$ K nm⁻².
 [25] Effective mass ratios inferred in the same way from magnetization data on the second ³He layer on bare graphite (C. Bauerle, Ph.D. thesis, Université Joseph Fourier, Grenoble, 1996) show a similar apparent divergence but displaced to a higher density, corresponding to the higher density of the $\sqrt{7} \times \sqrt{7}$ phase.
 [26] Y. Tokura *et al.*, Phys. Rev. Lett. **70**, 2126 (1993).
 [27] D. Coffey and K. S. Bedell, Phys. Rev. Lett. **71**, 1043 (1993).
 [28] M. Ogura and H. Namizawa, J. Phys. Soc. Jpn. **66**, 3706 (1997).
 [29] S. Misawa, J. Phys. Soc. Jpn. **68**, 2172 (1999).
 [30] D. S. Greywall, Phys. Rev. B **27**, 2747 (1983).
 [31] D. Coffey and C. Pethick, Phys. Rev. B **37**, 1647 (1988).
 [32] M. Imada, J. Phys. Soc. Jpn. **64**, 2954 (1995).
 [33] H. Kajueter, G. Kotliar, and G. Moeller, Phys. Rev. B **53**, 16214 (1996).